# Static shear stress of electrorheological fluids

G. L. Gulley and R. Tao
*Department of Physics, Southern Illinois University, Carbondale, Illinois 62901*
(Received 2 November 1992; revised manuscript received 2 June 1993)

We have calculated the static shear stress of an induced electrorheological solid for a single-chain structure, double-chain structure, triple-chain structure, and body-centered tetragonal (bct) lattice. When the shear strain is small, all of these four structures prefer slanted configurations which will come back to the original configurations if the load is removed. As the shear strain exceeds a yield point, the structures break into parts which cannot return to the original configurations in a short time. The bct lattice is found to have the strongest shear modulus. The triple-chain structure is weaker than the bct lattice, but much stronger than the single-chain structure and double-chain structure. The single-chain structure has the Peierls-Landau instability if the chain is very long. A double chain is stronger than a single chain if the chains are quite long and the situation is reversed if the chains are short.

PACS number(s): 82.70.Gg, 61.90.+d, 64.75.+g

## I. INTRODUCTION

An electrorheological (ER) fluid consists of a suspension of dielectric particles in a liquid of low dielectric constant [1–7]. When this suspension is exposed to an electric field, its viscosity increases dramatically. As the electric field exceeds a critical value, the suspension forms a solid whose shear modulus increases as the field is further strengthened. This phase transition is completed in about 1 ms and is reversible by reducing the electrical field past the critical field.

The understanding of the physical mechanisms of this phenomena is very important, since a wide variety of applications have been suggested for ER fluids. Some of these applications include suspension systems, valves, brakes, and clutches [1]. These alone will have a tremendous impact in the automobile and aerospace industries.

In this paper, we will discuss the static shear stress of the induced ER solid. The importance of shear stress is clear from the above applications. In experiments, it has been found that upon application of an electric field, the dielectric particles in ER fluids first form chains between two electrodes. Chains then aggregate to form thick columns [1]. Recent theoretical calculations and experiments have also shown that the ideal structure of the thick columns is a body-centered tetragonal (bct) lattice [3–5]. Since the static shear stress depends on the structure of the induced ER solid, we will calculate the shear stress for single chains, double chains, triple chains, and thick columns of the bct lattice.

Among the above four structures, which one is the strongest? This is an important issue to clarify. Some previous work claims that the double chains are weaker than the single chains and the structure consisting of single chains maximizes the shear stress [8]. This conclusion seems to contradict experimental results [9,10] and the well-known Peierls-Landau instability of a one-dimensional solid which implies a long single chain is a weak structure [3,11].

To resolve the above controversy, we have carried out the calculations which eventually show that the thick-column structure is much stronger than the single-chain structure. The triple-chain structure is stronger than the single-chain and double-chain structures and the bct lattice is even stronger than the triple-chain structure. The comparison between a single chain and a double chain depends on the chain length $L$. If the chains are long, the double chain is stronger than the single chain. Otherwise, the situation is reversed. These theoretical results are consistent with recent experimental measurement [9,10].

Our calculation also finds that when the shear strain is small, all of these four structures prefer slanted configurations which will come back to the original configurations if the load is removed. As the shear strain exceeds a yield point, the structures break into parts which cannot return to the original configurations in a short time. In extrapolating the shear modulus of the above four structures, we have found that the single-chain structure has its shear modulus tending to zero as the chain length $L$ goes infinite, a conclusion consistent with the Peierls-Landau instability. The other thicker structures seem to be stable as $L$ goes infinite. The yield point and structure-breaking in the deformation of an ER solid have been observed in experiments [9,10]. The response force and yield point derived from our calculation seem to agree with these experiments reasonably well.

The present paper is organized as follows. In Sec. II, we will discuss the dipolar interaction. Section III is devoted to the calculation of shear stress and shear modulus. The results and discussions are in Sec. IV, where we will also compare our theoretical results with experiments.

## II. DIPOLAR INTERACTION

We consider a model of ER fluids consisting of spherical particles of dielectric constant $\epsilon_p$ suspended in a fluid of dielectric constant $\epsilon_f, \epsilon_p > \epsilon_f$. This composite is subjected to an electric field inside a parallel plate capacitor whose two electrodes are planes at $z=0$ and $L$, respec-

 

tively. When the fluid is exposed to an electric field, the particles develop a dipole moment $\mathbf{p}$ in the direction of the electric field. Here $\mathbf{p}=\alpha\epsilon_f a^3\mathbf{E}_{\rm loc}$, where $a$ is the radius of the particles, $\alpha=(\epsilon_p-\epsilon_f)/(\epsilon_p+2\epsilon_f)$, and $\mathbf{E}_{\rm loc}$ is the local electric field.

To calculate the energy of this system of particles, we consider the dipole-dipole interactions. Two dipoles at $\mathbf{r}_i$ and $\mathbf{r}_j$ have an energy of

$$u(\mathbf{r}_{ij})=\nu(1-3\cos^2\theta_{ij})/r_{ij}^3 , \tag{2.1}$$

where $r_{ij}=|\mathbf{r}_i-\mathbf{r}_j|=[\rho^2+(z_i-z_j)^2]^{1/2}$, $\rho=\rho_{ij}=[(x_i-x_j)^2+(y_i-y_j)^2]^{1/2}$, $\theta_{ij}$ is the angle between their joint line and the direction of the applied field, and $\nu=\mathbf{p}^2/\epsilon_f$.

A dipole located at $(x,y,z)$ in a capacitor produces images at $(x,y,-z)$ and $(x,y,2Lj\pm z)$ for $j=\pm1,\pm2,\ldots$. The interaction between a dipole and its own image is $u(\mathbf{r}_{ij})/2$. The interaction between a dipole and a different dipole's images is $u(\mathbf{r}_{ij})$. All of these interactions must be summed to get the total energy of the interaction.

We introduce a function

$$f(\rho,z)=\sum_n[(2nL-z)^2+\rho^2]^{-3/2} . \tag{2.2}$$

A dipole at $\mathbf{r}_j$ and all its images interact with a dipole at $\mathbf{r}_i$ via

$$u_{ij}=-\nu\left[2+\rho\frac{\partial}{\partial\rho}\right][f(\rho,z_i-z_j)+f(\rho,z_i+z_j)] . \tag{2.3}$$

The interaction between a dipole inside the capacitor at $(x,y,z)$ with its infinite number of images at $(x,y,2Lj\pm z)(j=\pm1,\pm2,\ldots)$ is given by

$$u_s(z)=-\nu\zeta(3)/(4L^3)-\nu f(0,2z) , \tag{2.4}$$

where the constant $\zeta(3)=\sum_{n=1}^{\infty}1/n^3=1.202\,056\,9\ldots$. Because of the periodicity, $f(\rho,z)=f(\rho,z+2L)$, we can expand $f$ into the form $f(\rho,z)=\sum_{s=-\infty}^{\infty}f_s(\rho)e^{-is\pi z/L}$ with

$$\begin{aligned}f_s(\rho)&=\int_0^{2L}dz\,e^{is\pi z/L}f(\rho,z)/(2L)\\&=\pi sK_1(s\pi\rho/L)/(L^2\rho) ,\end{aligned} \tag{2.5}$$

where $K_1(\rho)$ is a modified Bessel function. Equation (2.2) now reads as

$$f(\rho,z)=1/(L\rho^2)+\sum_{s=1}^{\infty}2\pi sK_1(s\pi\rho/L)\times\cos(s\pi z/L)/(L^2\rho) . \tag{2.6}$$

The formula $d[xK_1(x)]/dx=-xK_0(x)$ enables us to write $u_{ij}$ in Eq. (2.3) as

$$u_{ij}(\rho_{ij},z_i,z_j)=\nu\sum_{s=1}^{\infty}(4s^2\pi^2/L^3)K_0(s\pi\rho_{ij}/L)\times\cos(s\pi z_i/L)\cos(s\pi z_j/L) . \tag{2.7}$$

## III. SHEAR STRESS AND SHEAR MODULUS

To apply a shear strain to the ER system, we move the electrode at $z=L$ along the $x$ direction by a distance $\delta$, while fixing the electrode at $z=0$. The shear strain is then $\delta/L$. We assume that there is no slipping between the electrodes and the induced ER structure. The slipping case has been studied in Ref. [4].

For a single chain under a shear strain we consider three configurations as illustrated in Figs. 1(a)–1(c). The slanted chain has each particle in the column moved along the $x$ direction proportionally. The broken chain has the chain broken into two parts in the middle with each part in the field direction. The slanted broken chain is broken in the middle but each part is still slanted. The separation of its two resulting parts $\delta_0$ is less than the deformation $\delta$ [Fig. 1(c)]. As we increase $\delta_0$, the slanted broken chain changes from the slanted chain to the broken chain.

Applying Eqs. (2.4) and (2.7), we have the total dipolar energies for a structure

$$\sum_j u_s(z_j)+\tfrac{1}{2}\sum_{\substack{i,j\\(i\neq j)}}u_{ij}(\rho_{ij},z_i,z_k) . \tag{3.1}$$

When the particle positions in Eq. (3.1) are for the slanted chain, slanted broken chain, and broken chain, we obtain $U_s(\delta)$, $U_{sb}(\delta)$, and $U_b(\delta)$, respectively. As shown in Fig. 2, $U_s(\delta)<U_b(\delta)$ until $\delta$ reaches a critical value $\delta_c$ where the curves for $U_s$ and for $U_b$ intersect. The slanted broken chain has an energy interpolating between the slanted chain and the broken chain. This implies that the slanted chain is preferred when the shear strain is less than $\delta_c/L$. However, when the shear strain exceeds $\delta_c/L$, the broken chain has the lowest energy and the slanted broken chain has its energy higher than that of

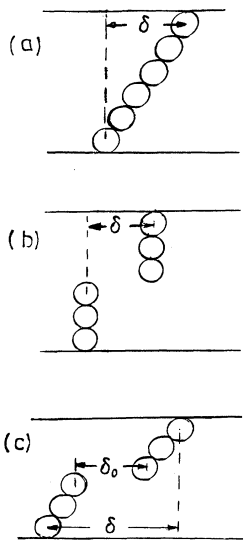


FIG. 1. (a) Slanted single chain. (b) Broken single chain. (c) Slanted-broken single chain.

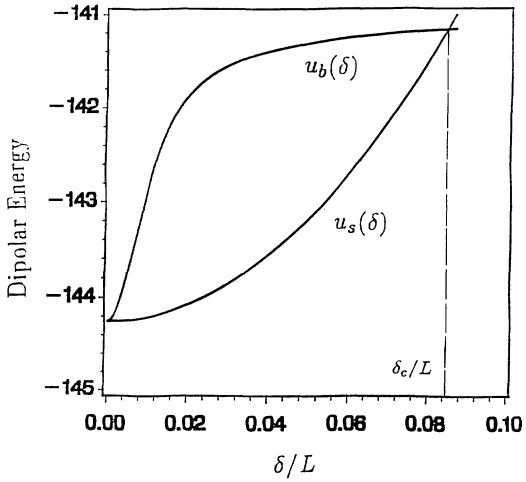


FIG. 2. The dipolar energies of the slanted single chain and the broken single chain vs the shear strain, respectively. The single chain has 60 particles. When $\delta < \delta_c$, the slanted chain is preferred. When $\delta > \delta_c$, the broken chain is preferred. The energy unit is $p^2/(\epsilon_f d^3)$.

the broken chain and lower than that of the slanted chain. Therefore, the competition is really between the slanted chain and the broken chain. When the shear strain is greater than $\delta_c/L$, the chain suddenly breaks into two parts. There is no intermediate state. For this reason, $U_{sb}$ is not plotted in Fig. 2.

When $\delta < \delta_c$, the response force per chain is given by

$$\tau = -\frac{\partial U_s(\delta)}{\partial \delta} . \tag{3.2a}$$

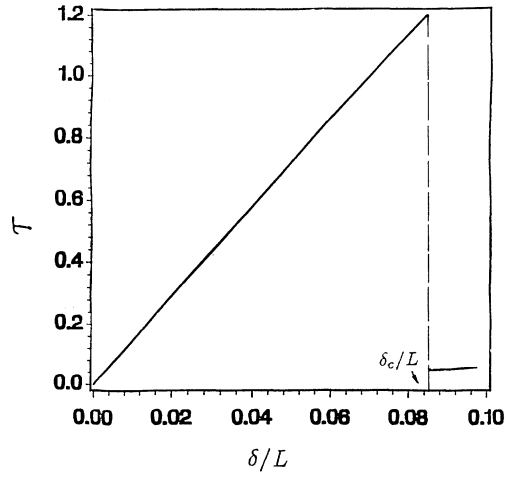


FIG. 3. The response force of a single chain of 60 particles vs the shear strain. When $\delta < \delta_c$, the slanted chain produces $\tau$ almost linear with $\delta/L$. When $\delta > \delta_c$, the preferred broken chain produces a much smaller and almost flat $\tau$. The force unit is $p^2/(\epsilon_f d^4)$.

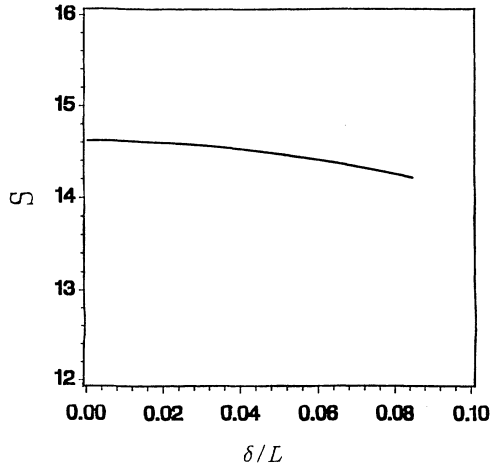


FIG. 4. The response coefficient $S$ of a single chain of 60 particles vs the shear strain up to the yield point. The unit of $S$ is $p^2/(\epsilon_f d^4)$.

When $\delta > \delta_c$, the response force per chain is given by

$$\tau = -\frac{\partial U_b(\delta)}{\partial \delta} . \tag{3.2b}$$

Figure 3 shows the behavior of the response force of a single chain versus the shear strain $\delta/L$. When $\delta < \delta_c$, the slanted chain gives a response force $\tau_s$ almost linear with $\delta/L$. When $\delta > \delta_c$, the preferred broken chain produces a much smaller and almost flat response force. The unit of $\tau$ in our calculation is $p^2/(\epsilon_f d^4)$ where $d = 2a$, the particle diameter.

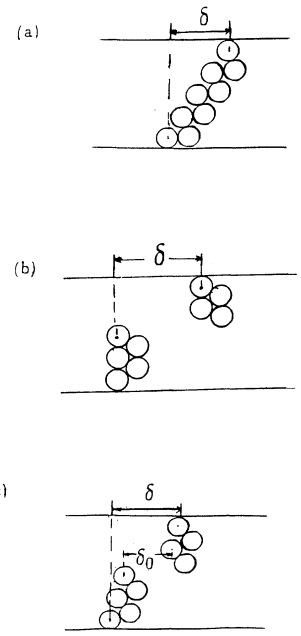


FIG. 5. (a) Slanted double chain. (b) Broken double chain. (c) Slanted-broken double chain.

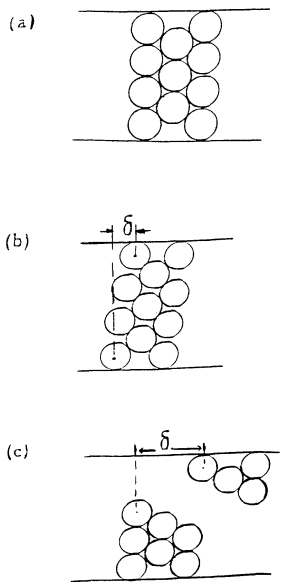


FIG. 6. (a) Triple-chain structure. (b) Slanted triple chain. (c) Broken double chain.

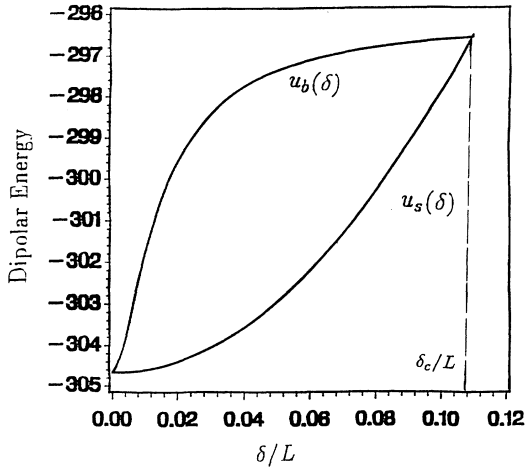


FIG. 8. The dipolar energies of the slanted double chain and the broken chain vs the shear strain, respectively. When $\delta < \delta_c$, the slanted double chain is preferred. When $\delta > \delta_c$, the broken double chain is preferred. The double chain has 119 particles. The energy unit is $p^2/(\epsilon_f d^3)$.

A single chain has $N = L/d$ particles. At a volume fraction $\phi$, for the structure consisting of single chains, the number of chains per unit cross area is $6\phi/(\pi d^2)$. The shear modulus of the single-chain structure at volume fraction $\phi$ is $6\phi S/(\pi d^2)$, where $S$ is the response coefficient, given by

$$S = \tau L/\delta \ . \tag{3.3}$$

In Fig. 4 we plot $S$ versus shear strain $\delta/L$ up to $\delta_c/L$. When $\delta > \delta_c$, it is clear from Fig. 3 that the broken chain has a much smaller $S$.

The quantity $\delta_c/L$ is of special interest. When the shear strain is small, the slanted chain represents a state which has a uniform deformation. The response force is approximately proportional to the shear strain (Fig. 3) and the response coefficient is almost a constant (Fig. 4). The single chain will recover its original shape as soon as the shear stress is removed. When $\delta$ becomes greater than $\delta_c$, the chain suddenly breaks. The broken chain is the state in which there is structural damage. We expect that as $\delta > \delta_c$, the chain cannot recover its initial single chain configuration in a short time. Therefore, $\delta_c/L$ is a yield point. The critical response coefficient of a single chain at $\delta_c/L$ is given by

$$S_c = \tau_c L/\delta_c \ , \tag{3.4}$$

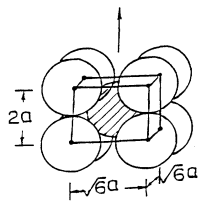


FIG. 7. Three-dimensional bct lattice.

where $\tau_c$ is the response force at the yield point. The critical shear modulus of the single-chain structure is $6\phi S_c/(\pi d^2)$. It is clear that the critical response coefficient per particle $S_c/N$ provides a measure of the structure strength. The larger the $S_c/N$, the stronger the structure.

The same calculations and analysis are carried for double chains, triple chains, and thick columns of the bct lattice. These structures are formed by two different chains. As shown in Fig. 5(a), a chain of class $A$ has particles extending the full length of the capacitor. A chain of class $B$ can be obtained by moving a chain of class $A$ in the $z$

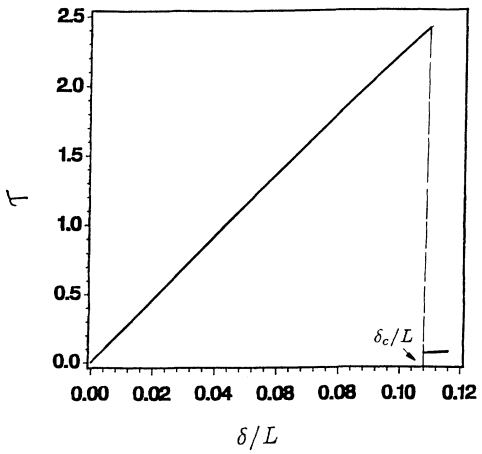


FIG. 9. The response force of a double chain of 119 particles vs the shear strain. When $\delta < \delta_c$, the slanted double chain produces a $\tau$ almost linear with $\delta/L$. When $\delta > \delta_c$, the preferred broken double chain produces a much smaller and almost flat $\tau$. The force unit is $p^2/(\epsilon_f d^4)$.

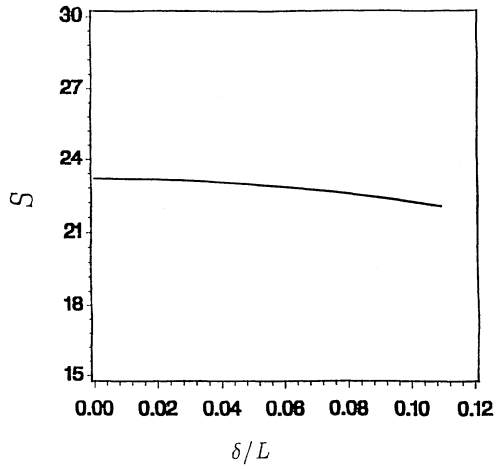


FIG. 10. The response coefficient $S$ of a double chain of 119 particles vs the shear strain up to the yield point. The unit of $S$ is $p^2/(\epsilon_f d^4)$.

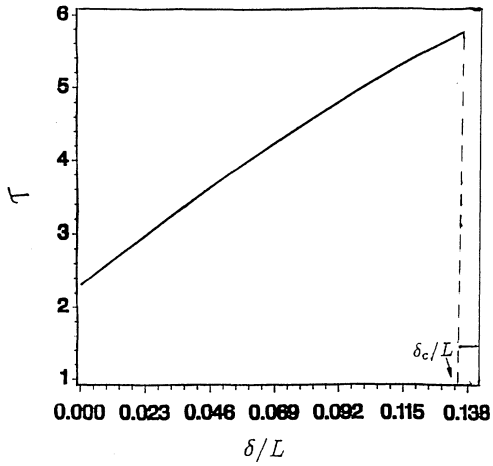


FIG. 12. The response force of a triple chain of 59 particles vs the shear strain. When $\delta < \delta_c$, the slanted structure produces a $\tau$ almost linear with $\delta/L$. When $\delta > \delta_c$, the preferred broken structure produces a much smaller and almost flat $\tau$. The force unit is $p^2/(\epsilon_f d^4)$.

direction by a sphere radius. In addition, because of the two electrodes, a chain of class $A$ has $L/d$ particles, while a chain of class $B$ has $(L/d-1)$ particles. A double chain has one $A$ chain and one $B$ chain closely packed. Its three configurations under a shear strain, slanted double chain, broken double chain, and slanted-broken double chain are shown in Fig. 5(a)–5(c).

As shown in Fig. 6(a), the triple chains are formed from two $A$ chains and one $B$ chain closely packed. The slanted triple chain and broken triple chain are plotted in Figs. 6(b) and 6(c). A thick column of the bct lattice is a three-dimensional structure, shown in Fig. 7. We denote its three conventional Bravais lattice vectors as $\sqrt{3}a(\hat{\mathbf{x}}+\hat{\mathbf{y}})$, $\sqrt{3}a(\hat{\mathbf{x}}-\hat{\mathbf{y}})$, and $2a\hat{\mathbf{z}}$ (see Fig. 7). This structure can also be considered as a compound of $A$ chains and $B$ chains [5]. There are four $A$ chains around one $B$ chain.

Figure 8 gives the dipolar energies of the slanted double chains and broken double chains of 119 particles. Figure 9 shows the response force $\tau$ of this double chain. Figure 10 is its response coefficient $S$. At volume fraction $\phi$, the double-chain structure has $6\phi/[\pi d^2(2-d/L)]$ double chains per unit cross section. Therefore, this double chain structure has shear modulus $6S\phi[\pi d^2(2-d/L)]$.

Figure 11 gives the dipolar energies of the slanted and broken triple chain of 59 particles. Figures 12 and 13 show the response force and response coefficient of this triple chain.

The bct lattice used in our calculation has nine $A$ chains and four $B$ chains. Since a bct lattice is a noniso-

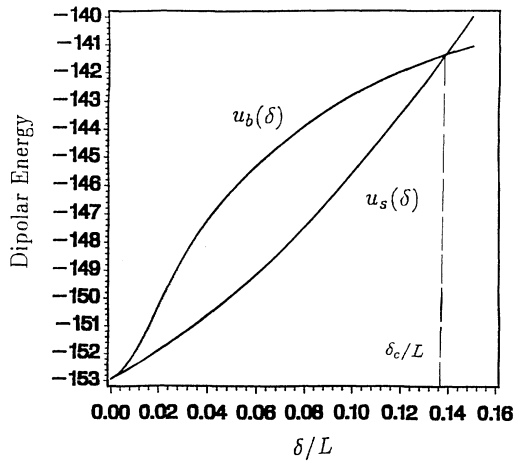


FIG. 11. The dipolar energies of the slanted triple chain and the broken chain vs the shear strain, respectively. The triple chain has 59 particles. When $\delta < \delta_c$, the slanted triple chain is preferred. When $\delta > \delta_c$, the broken triple chain is preferred. The energy unit is $p^2/(\epsilon_f d^3)$.

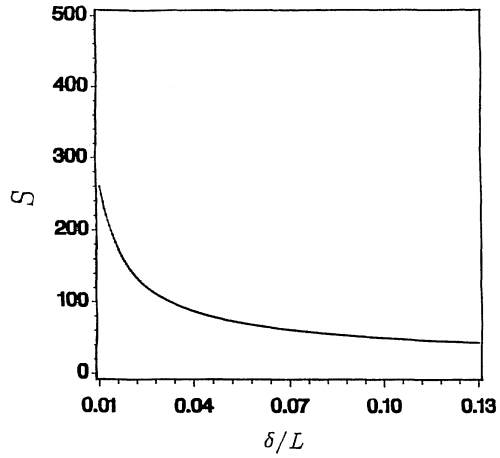


FIG. 13. The response coefficient $S$ of a triple chain of 59 particles vs the shear strain. The unit of $S$ is $p^2/(\epsilon_f d^4)$.

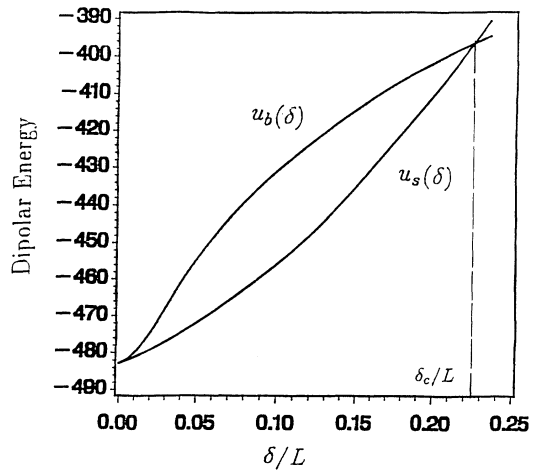


FIG. 14. The dipolar energies of the slanted bct lattice and the broken bct lattice vs the shear strain, respectively. The bct lattice has 178 particles. When $\delta < \delta_c$, the slanted structure is preferred. When $\delta > \delta_c$, the broken structure is preferred. The energy unit is $p^2/(\epsilon_f d^3)$.

tropic three-dimensional structure, we first compared deformations in different directions. It turns out that the shear strain in the $x$ (or $y$) direction has the lowest response force for this bct lattice. In Fig. 14, we plot the dipolar energies of the slanted and broken bct lattice of 178 particles which has 9 $A$ chains, 14 particles each, and 4 $B$ chains, 13 particles each. Figure 15 depicts the response force $\tau$ for the bct lattice. Figure 16 shows the response coefficient $S$ of this bct lattice. All deformations in Figs. 14–16 are in the $x$ direction.

Similar to the single-chain case, there is a yield point $\delta_c/L$ for all of these structures. when the shear strain is less $\delta_c/L$, the slanted structures are always preferred.

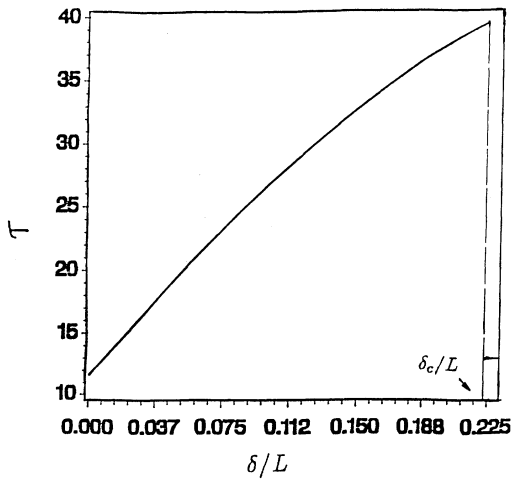


FIG. 15. The response force of a bct lattice of 178 particles vs the shear strain. When $\delta < \delta_c$, the slanted structure produces a $\tau$ almost linear with $\delta/L$. When $\delta > \delta_c$, the preferred broken structure produces a much smaller and almost flat $\tau$. The force unit is $p^2/(\epsilon_f d^4)$.

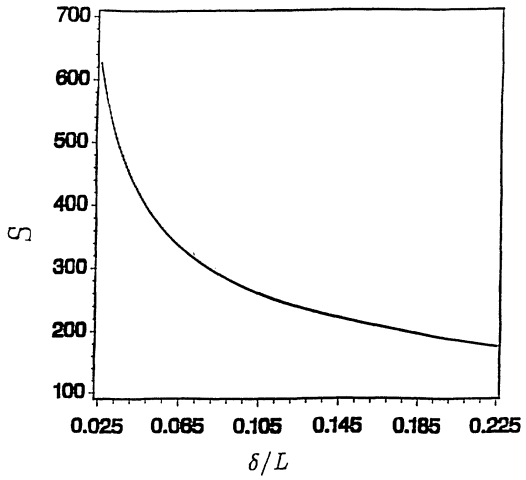


FIG. 16. The response coefficient $S$ of the bct lattice of 178 particles vs the shear strain up to the yield point. The unit $S$ is $p^2/(\epsilon_f d^4)$.

When the shear strain exceeds $\delta_c/L$, the structures break into two parts. The slanted broken structures always have an energy interpolating between the slanted structures and the broken structures. Therefore, the competition is really between the slanted structures and the broken structures. As seen in Figs. 9, 12, and 15, similar to a single chain, when $\delta > \delta_c$, the preferred broken structures produce a much smaller and almost flat response force. In Figs. 10, 13, and 16, we plot the response coefficient $S$ of these thick structures up to their yield point. It is clear from Figs. 9, 12, and 15 that all of these structures have a much smaller $S$ beyond the yield point.

As in Eq. (3.4), the critical response coefficient per particle $S_c/N$ of the double chain, triple chain, and the bct lattice provides measurement of the strength of the induced structures.

## IV. RESULTS AND DISCUSSIONS

To understand the stability of the solid structures and make a comparison, we plot the critical response coefficients per particle $S_c/N$ versus $d/L$ in Fig. 17. As stated earlier, the higher $S_c/N$, the stronger the structure.

Figure 17 first shows that a single chain is stronger than a double chain when $L/d$ is small. This is consistent with the result reported in Ref. [8]. However, as $L/d$ increases (or as $d/L$ decreases in Fig. 17), the critical response coefficient of a double chain decreases slower than that of a single chain. When $L/d > 400$, a double chain becomes stronger than a single chain. Our numerical calculation also verifies this conclusion.

In addition, as $d/L \to 0$, the critical response coefficient per particle of a single chain tends to zero. This is the Peierls-Landau instability of an infinite one-dimensional solid. As seen from Fig. 17, the response coefficients per particle of a double chain, triple chain, and bct lattice do not extrapolate to zero as $d/L \to 0$. This implies that these thick structures are more stable

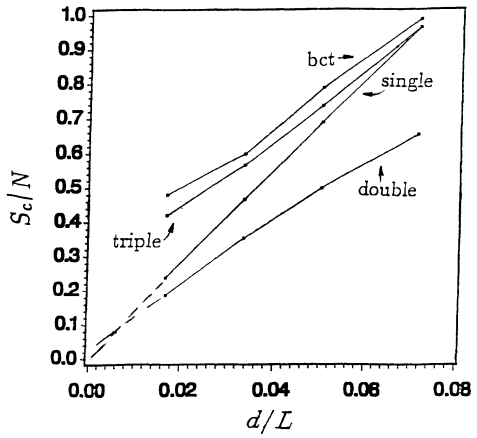


FIG. 17. Critical response coefficient per particle vs $d/L$ for the single chain, double chain, triple chain, and bct lattice.

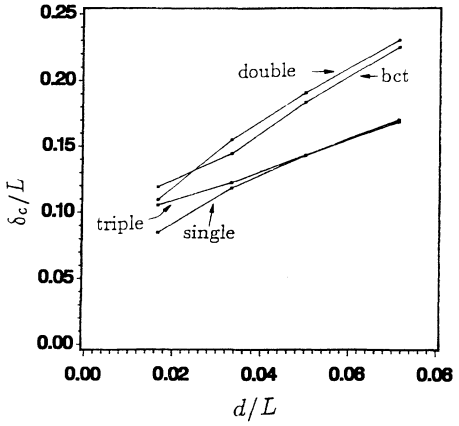


FIG. 18. Yield point $\delta_c/L$ vs $d/L$ for the single chain, double chain, triple chain, and bct lattice.

than the single-chain structure. The single-chain structure may be stable only if the electrode spacing is not too wide.

As seen from Fig. 17, the triple chain is much stronger than the double chain. When $L=60d$, the critical response coefficient per particle of a triple chain is twice as large as that of a double chain. The bct lattice is even stronger than the triple-chain structure.

Figures 13 and 16 also show that the response force of a triple chain and a bct lattice is not linear with a small deformation $\delta$. These structures are closed packed and have very limited room to move their particles (Fig. 7). In responding to the initial deformation, they usually produce a quite large modulus to resist the deformation. For example, a triple chain in Fig. 6(a) has two chains of class $A$ and one chain of class $B$. During deformation, the positions of the second chain of class $A$ is affected by the deformation of the middle chain of class $B$. If $\delta$ increases, the deformed structures are no longer close packed; and then there is more room to arrange particles and the response force becomes almost linear with the deformation. Therefore, the response coefficient of a triple chain and a bct lattice is very high for small $\delta$ and then it decreases with an increase of $\delta$ and tends to be stable as $\delta$ further increases until $\delta_c$ is reached.

Because the single-chain structure is not a close-packed structure (Fig. 1), its response force is almost linear to the deformation from the beginning as seen in Fig. 4. Though a double chain has a single chain of class $A$ and a single chain of class $B$ close packed, the geometric deformation of these two chains is not affected by each other as in a triple chain or bct lattice (Fig. 5). Therefore, the response force is also almost linear to the deformation from the beginning.

In Fig. 18 we plot the yield point $\delta_c/L$ versus $d/L$ for all four structures. It is noted that as $L/d$ increases, the yield point decreases. As $d/L\rightarrow 0$, the critical shear strain of a single chain does not tend to zero. This implies that to break a long single chain, a minimum shear strain is still needed, though the shear modulus is vanishing.

To conclude our paper, we would like to make some comparison of our theoretical results with experiments [9]. Conrad, Sprecher, and Chen observed the single-chain structure when $\phi$ is low and $L/d$ is not too large. Similar to our discussion, they applied a shear strain to the chain by sliding one electrode. The sliding electrode had a rough surface and there was sticking between the electrode and particles. The same as in our theoretical discussion, the chain first became slanted, then broke into two parts when the shear strain exceeded a yield point. For example, their experiment found the yield point $\delta_c/L$ was about 0.4 for $L/d=3$. Our calculation finds $\delta_c/L=0.31$ for $L=3d$, close to the experimental results. Their experiment also found the response force was about $3.8\times10^{-6}N$ for shear strain 0.21, $L/d=3$, and $E=2$ kV/mm. Our calculation has the response force $3.0p^2/(\epsilon_f d^4)$ under the above condition. The dielectric particles in the experiment were moist glass spheres of $d=150$ $\mu$m. The liquid has $\epsilon_f=2.5$. The effective dielectric constant of moist glass spheres was not measured in the experiment but was expected to be higher than 7.2, the dielectric constant of dry glass spheres. Applying the effective local field for a single chain [5],

$$E_{\rm loc}=E/(1-0.601\,028\alpha)\ , \tag{4.1}$$

we have found our response force close to $3.8\times10^{-6}N$ when $\epsilon_p=22.8$, a reasonable result for the effective dielectric constant of moist glass spheres.

In another experiment [10], the above group found that when the volume fraction $\phi<0.06$, the measured shear stress was consistent with the shear stress of a single-chain structure. When $\phi>0.06$, double chains were formed and the measured shear stress was stronger than that of the single-chain structure. As $\phi$ was further increased, the measured shear stress increased because thick columns were formed. This conclusion matches our theoretical calculation.

Worthy of note is that our present calculation is based on the dipolar approximation. Though we include the local field as in Eq. (4.1) to improve our results, the contribution from higher multipoles is not negligible when the volume fraction $\phi$ is high [12,13]. Then the response

force will be stronger than that under the dipolar approximation. In addition, the thick structures are even more favorable in ER fluids when $\epsilon_p > \epsilon_f$ [12,13]. It is also for this reason that we should expect the experiments to find the double-chain structure, triple chain structure, and bct lattice structure stronger than that from our calculation.

## ACKNOWLEDGMENTS

This research is supported by the Office of Naval Research Grant No. N00014-90-J-4041 and a grant from Materials Technology Center of Southern Illinois University at Carbondale.

[1] For example, see *Electrorheological Fluids,* edited by R. Tao (World Scientific, Singapore, 1992); P. M. Adriani and A. P. Gast, Faraday Discuss. Chem. Soc. **90**, 1 (1990); W. M. Winslow, J. Appl. Phys. **20**, 1137 (1949); H. Block and J. P. Kelly, U.S. Patent No. 4 687 589 (1987); J. D. Carlson, U.S. Patent No. 4 772 407 (1988); F. E. Filisko and W. E. Armstrong, U.S. Patent No. 4 744 914 (1988); D. J. Klingenberg, F. van Swol, and C. F. Zukoski, J. Chem. Phys. **91**, 7888 (1989).

[2] R. Tao, J. T. Woestman, and N. K. Jaggi, Appl. Phys. Lett. **55**, 1844 (1989).

[3] T. C. Halsey and W. Toor, Phys. Rev. Lett. **65**, 2820 (1990).

[4] T. C. Halsey, J. E. Martin, and D. Adolf, Phys. Rev. Lett. **68**, 1519 (1992).

[5] R. Tao and J. M. Sun, Phys. Rev. Lett. **67**, 398 (1991).

[6] R. Tao and J. M. Sun, Phys. Rev. A **44**, R6181 (1991).

[7] T. J. Chen, R. N. Zitter, and R. Tao, Phys. Rev. Lett. **68**, 2555 (1992).

[8] A. M. Kraynik, R. T. Bonnecaze, and J. F. Brady, in *Electrorheological Fluids* (Ref. [1]), p. 59.

[9] H. Conrad, A. F. Sprecher, and Y. Chen, in *Electrorheological Fluids,* edited by J. D. Carlson, A. F. Sprecher, and H. Conrad (Technomic, Lancaster, PA, 1990) p. 82.

[10] H. Conrad, A. F. Sprecher, and Y. Chen, in *Electrorheological Fluids* (Ref. [1]), p. 195.

[11] L. D. Landau, in *Collected Papers of L. D. Landau,* edited by D. ter Haar (Gordon and Breach, New York, 1965), p. 209; R. E. Peierls, Helv. Phys. Acta Suppl. **7**, 81 (1934).

[12] L. C. Davis, Appl. Phys. Lett. **60**, 319 (1992); J. Appl. Phys. **72**, 1334 (1992).

[13] Y. Chen, A. F. Sprecher, and H. Conrad, J. Appl. Phys. **70**, 6796 (1991).